

# One-dimensional dimer chain for topological wireless power transfer

Fengqing Yang, Juan Song, Zhiwei Guo\*, Youqi Chen, Haitao Jiang, Yunhui Li, and Hong Chen

*Key Laboratory of Advanced Micro-structure Materials, MOE, School of Physics Science and Engineering, Tongji University,*

*Shanghai 200092, China*

## Abstract

Manipulating the topological phase transition of the photonic insulators will provide a unique control for the interaction between light and matter, such as the exotic edge states with topological protection. To date, the topological characteristics including invariant topological orders, band inversion, and the edge states in the photonic insulators have been widely studied and experimentally demonstrated. Whether people can take advantage of intriguing topological states in simple one-dimensional systems to implement some practical applications is an issue which people are increasingly concerned about. Specially, the edge states in the topological dimer chain have been proposed to realize the topological robust lasers. In this work, based on a photonic dimer chain composed of ultra-subwavelength resonators, we verify experimentally that the topological edge state is immune to the inner disorder perturbation and can be used to realize the wireless power transfer (WPT) with high transmission efficiency. This property of high transmission efficiency can be guaranteed even when the length of chain changes. Moreover, to intuitively show the topological edge state can be used for WPT, a power signal source is used to excite the topological edge state. It can be clearly seen that the LED lamps with 0.5-W at both ends of the structure corresponding to the edge state are lighted up. Inspired by the long-range WPT implemented by the edge state in this work, it is expected to use more complex topological structures to achieve more functional energy transmission, such as the WPT whose direction can be selected flexibly in the quasiperiodic topological Harper chain.

**Keywords:** topological edge states; Su-Schrieffer-Heeger model; wireless power transfer.

\* Corresponding author: Email: [2014guozhiwei@tongji.edu.cn](mailto:2014guozhiwei@tongji.edu.cn)

## INTRODUCTION

Photonic artificial topological structures provide a good platform for people to study the electromagnetic wave manipulation [1-3]. To date, a large number of photonic topological structures, including metamaterials [4-7], coupled ring arrays [8-11], local resonant arrays [12-14], circuit networks [15-17], and photonic crystals [18-24], have been used to study the abundant topological excitations [25-27]. By mapping the basic topological Su-Schrieffer-Heeger model of a solid-state system [28], the photonic one-dimensional (1D) dimer chain has been demonstrated to realize the topological edge states which are robust against the disorder and fluctuations. Notably, in 2009 Malkova et al. experimentally reveal that the linear Shockley-like surface states in an optically induced semi-infinite photonic superlattice and it is the first demonstration of 1D topological states in photonics [29]. Recently, the topological phase transition, invariant topological orders and the associated edge states in the topological dimer chain have been experimentally observed in the platform composed of split-ring resonators in microwave regime [30, 31]. The great progress of the topological dimer chains has enabled some interesting extensions to be realized along with some important applications [32]. On the one hand, research on the advantages of 1D dimer chains has been extended to nonlinear [33-35] and active [36, 37] systems, where the active controlled topological edge states and topological lasers are studied respectively. On the other hand, the topological properties of non-Hermitian dimer chain have been theoretically studied and experimentally demonstrated [38-42]. Especially, combining the non-Hermitian exceptional points (EPs) with topological

states, a new sensor which is not sensitive to internal manufacturing errors but is highly sensitive to changes in the external environment is proposed [43]. Although the structure of 1D photonic dimer chain is simple, its fertile topological physical and useful applications have attracted more and more attention.

In this work, using the ultra-subwavelength coil resonators, the 1D dimer chain under the tight-binding model is designed and fabricated. Moreover, we apply the edge state in the topological chain to a specific application scenario — wireless power transfer (WPT) [44-47]. Normally, traditional WPT devices with magnetic induction mechanism are usually limited by the transmission distance [48-51]. When the distance between the receiving coil and the transmitting coil is large enough, the transmission efficiency will be greatly reduced. As an effective solution, magnetic resonance WPT can achieve long-range and efficient energy transmission [52-63]. However, the associated frequency tracking is also an important problem in practical applications [64-66]. Here, we propose the long-range WPT of topological edge state with high transmission efficiency. Firstly, because the edge states are symmetrically localized at both ends of the topological dimer chain, the long-range WPT can be achieved by choosing different chain lengths according to the actual needs. Secondly, for a long 1D dimer chain, the frequency position of the topological edge state is fixed. Therefore, the working frequency will not be changed due to the change of transmission distance, which provides a new scheme for dynamic WPT. Finally, given the topological edge state, the designed WPT device will be robust to the disorder perturbation inside the structure, which makes our new WPT device have high stability in complex

transmission scenarios. Our results provide a versatile platform to design the WPT devices with topological protection. Considering the asymmetric edge states in the quasiperiodic [67] or the trimer [68] topological chain, our platform is expected to further realize the interesting and directional WPT in the future.

## RESULTS

In the experiment, the 1D topological dimer chain is constructed by ultra-subwavelength coil resonators. The composite coil resonator is composed of two layers divided by a polymethyl methacrylate (PMMA) substrate with thickness of  $h = 1$  cm. The top layer corresponds to a coil resonator and the photo is shown in Fig. 1(a). All the coil resonators in the dimer chain are identical with the resonant frequency of  $f_0 = 5.5$  MHz, which depends on the loaded lumped capacitor  $C = 100$  pF and the geometric parameters including the inner diameter  $D_1 = 5.2$  cm and outer diameter  $D_2 = 7$  cm. The Fig. 1(b) shows the back layer of the composite resonator, in which a 0.5-W LED lamp is connected to a non-resonant coil. Once the magnetic field in the top coil is strong enough, the LED lamp loaded in the back layer can be lighted up. Fig. 1(c) shows the 1D dimer chain with  $Nc$  unit cells. Based on the tight-binding model, the Hamiltonian of the photonic dimer chain can be written as follows [28]:

$$H = \sum_n (\kappa_1 a_n^\dagger b_n + \kappa_2 a_{n+1} b_n^\dagger) + h.c. , \quad (1)$$

where  $\kappa_1$  and  $\kappa_2$  respectively denote the intra-cell coupling and inter-cell coupling coefficients, which are controlled by tuning the distance between coil resonators [67, 68]. In our photonic dimer chain, the distance of intra-cell and inter-cell are 4 cm and 3 cm, respectively.  $a_n(b_n)$  and  $a_n^\dagger(b_n^\dagger)$  represent the generation and annihilation

operators corresponding to  $a(b)$  lattice point in the  $n^{\text{th}}$  unit cell of SSH chain, respectively. The topological invariants of the system can be determined by Zak phase of the band [28]:

$$v = \int_{-\pi}^{\pi} i \left\langle u_k \left| \frac{\partial}{\partial k} \right| u_k \right\rangle dk, \quad (2)$$

where  $u_k$  is the eigenvector. The Zak phase trivial chain ( $\kappa_1 > \kappa_2$ ) and topological chain ( $\kappa_1 < \kappa_2$ ) are  $v = 0$  and  $v = \pi$ , respectively. The edge states will appear symmetrically at two ends of the chain for the topological dimer chain.

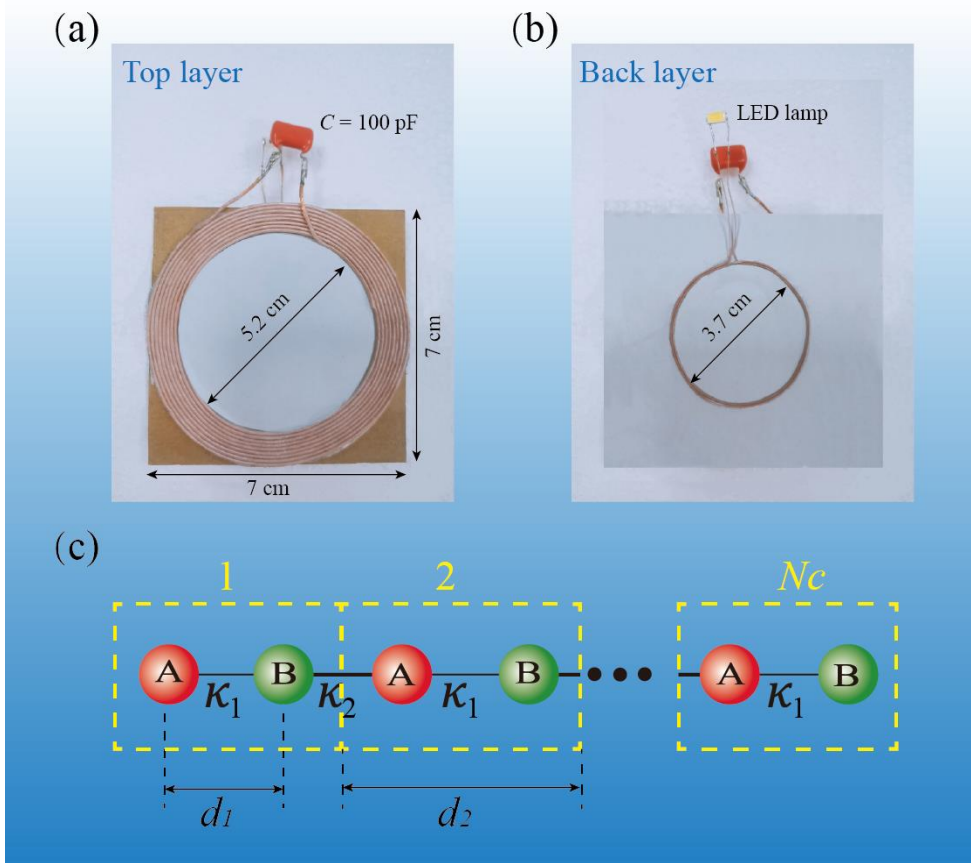


FIG. 1. **Details of the composite resonator and the 1D dimer chain.** (a) The resonator on the top layer of the composite structure. Here, the resonant frequency of the coil is 5.5 MHz; the loaded capacitor is 100 pF; the thickness of the substrate is 1 cm; the inner diameter and outer diameter of the coil resonator are 5.2 cm and 7cm, respectively. (b) A non-resonant coil with a LED lamp on the back layer of the composite structure. The corresponding diameter of the non-resonant coil is 3.7 cm. (c) Schematic of the 1D dimer chain. In this tight-binding model, the unit cell is composed of two resonators, which are marked by red and green respectively, to facilitate viewing.

Based on the near-field detection method [30, 31], we measure the density of states (DOS) spectrum of the topological chain composed of 16 coil resonators. Our near-field magnetic probe is a loop antenna, which is connected to the port of the vector network analyzer (Agilent PNA Network Analyzer N5222A). The radius of the loop probe is 2 cm. It can be taken as a non-resonant antenna with high impedance. This small loop antenna acts as a source to excite the sample and then measure the reflection. And the local density of states (LDOS) of each site is obtained from the reflection by putting the probe to the center of the corresponding resonator. The DOS spectrum is obtained by averaging the LDOS spectral over all 16 sites. The measured DOS spectrum of the topological dimer chain without disorder perturbation is shown in Fig. 2(a). An isolated state ( $f = 5.62$  MHz) exists in the bandgap of the spectrum, which belongs to the edge state colored by red arrow. To investigate the robustness of the edge states against disorder perturbation, we randomly move 10 coil resonators 5mm in the center of the topological dimer chain. The corresponding measured DOS spectrum of the topological dimer chain with disorder perturbation is shown in Fig. 2(b). Comparing Figs. 2(a) and 2(b) shows that, the edge state is still maintained for the dimer chain with perturbation whereas the bulk state has been deteriorated seriously.

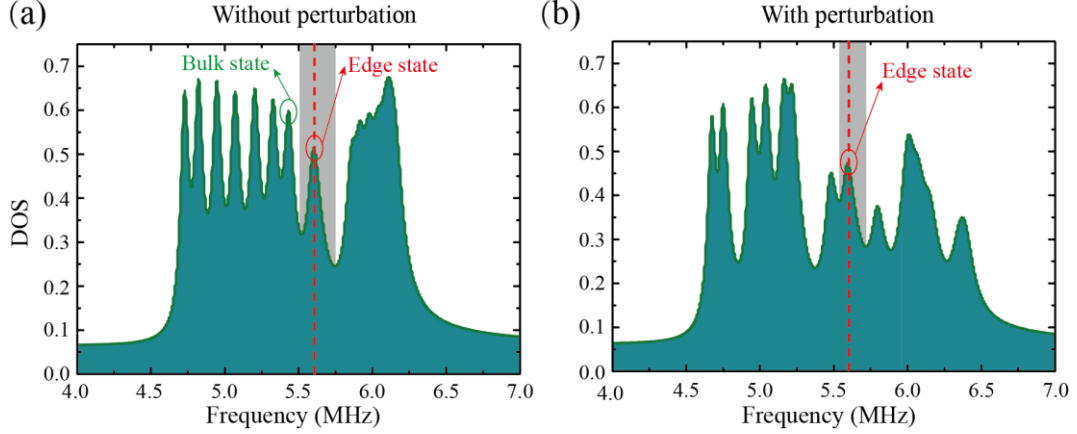


FIG. 2. **Measured DOS spectrum of the 1D topological dimer chain.** (a) Measured DOS spectrum of the 1D topological dimer chain without perturbation. One bulk state ( $f = 5.43$  MHz) and the edge state ( $f = 5.62$  MHz) in the band gap are marked by the green arrow and red arrow, respectively. (b) Similar to (a), but for the case with disorder perturbation in the inner of the chain. The structure disorder is realized by randomly moving the central 10 resonators with 5 mm.

Moreover, we measure the LDOS distributions of the edge state and one bulk state, which are marked by red and green arrows in Fig. 2, respectively. For the bulk state in the band, the LDOS is mainly distributed in the bulk, as shown in Fig. 3(a). When the dimer chain with disorder perturbation, the LDOS of the bulk state is significantly modified in Fig. 3(b). However, for the dimer chain with disorder perturbation, the measured LDOS of the edge state is still confined at the two ends of the chain in Fig. 3(d), just as the case without perturbation in Fig. 3(c). This indicates that when random movement is introduced into the interior of the chain, the topological edge state will not be modified, which is highly significant for robust WPT.

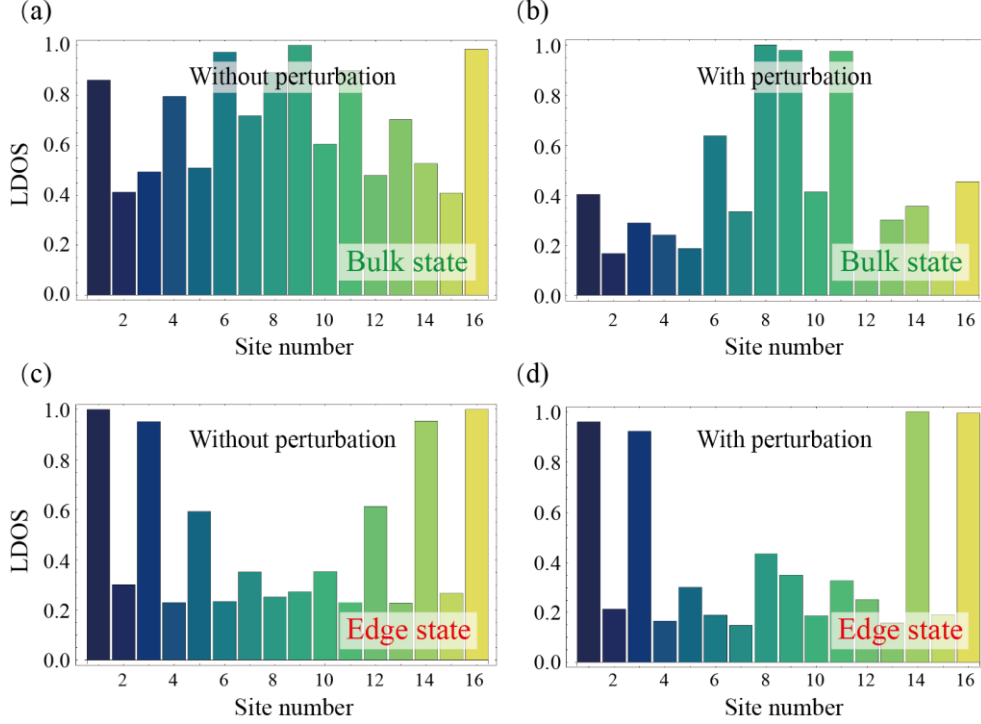
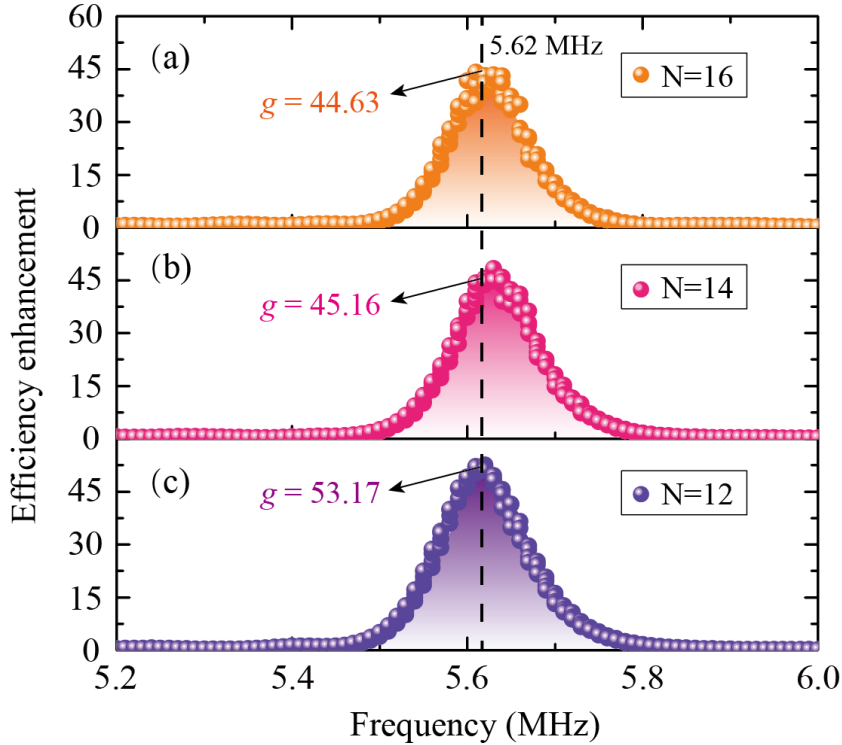


FIG. 3. **Robust edge state against the disorder perturbation.** (a) Measured normalized LDOS distribution of the bulk state (marked by green arrow in Fig. 2(a)) in the topological dimer chain without perturbation. (b) Similar to (a), but for the LDOS distribution of the bulk state with disorder perturbation. (c) (d) Measured normalized LDOS distribution of the edge state in Figs. 2(a) and 2(b), respectively.

At present, the WPT system of magnetic resonance has been demonstrated to be the powerful tools to improve the functionalities and obtain new performance beyond the WPT systems of magnetic induction. In particular, magnetic resonance WPT can achieve long-range and efficient transmission [52-63]. However, the transmission efficiency of magnetic resonance WPT tightly depends on the transmission distance. The effective working frequency needs to be changed with the transmission distance because of the near-field coupling mechanism, which limits its practical applications. To solve this problem, an optimization scheme is proposed, which uses nonlinear effect to track the real-time working frequency [64-66]. For frequency tracking WPT system, the power carrying capacity of nonlinear circuit elements will limit the upper limit of transmission power of the whole energy transmission system. Here, based on the

topological edge state in the dimer chain, we realize that the long-range WPT is independent on transmission distance. It is mainly because when the dimer chain gets longer, the working frequency of the topological state can be kept fixed, which almost is independent on the transmission distance. **Figures 4(a)-4(c)** show the measured enhancement of transmission efficiency of topological chain over trivial chain when the length of the chain changed. It can be clearly seen that the position of topological state hardly changes with the chain length. For the topological dimer chain with 16, 14, and 12 coil resonators, the efficiency enhancement at the working frequency of 5.62 MHz is always high. Therefore, the topological state can be used for long-range WPT without the influence of distance.



**FIG. 4. Measured enhancement of transmission efficiency of topological chain over trivial chain when the length of the chain changed.** (a) The transmission efficiency of a topological chain divided by that of a trivial chain when the number of the resonators in the chain is  $N=16$ . (b) (c) Similar to (a), but for the number of the resonators in the chain is  $N=14$  and  $N=12$ , respectively. At the working frequency  $f = 5.62$  MHz, the efficiency enhancement in three chains with  $N=16$ , 14, and 12 correspond to  $g = 44.63$ , 45.16 and 53.17, respectively.

At the end of this work, the experiment is carried out to exhibit an actually high-power WPT control. The high-power signal source (AG Series Amplifier, T&C Power Conversion) instead of the vector network analyzer, is used to excite the topological edge states. A source non-resonant coil is placed in the center of the structure. To show the topological WPT intuitively, except for the two resonators near the source coil, all other resonators are added with LED lamps. At the working frequency of topological edge state, the LED lamps on both sides of the chain are lighted up whereas the LEDs lamps loaded on other composite resonators remain dark, which is shown in Fig. 5. Considering the asymmetric field pattern of topological edge state in quasiperiodic chain, the unidirectional WPT may also be realized by our setup based on the coil resonators.

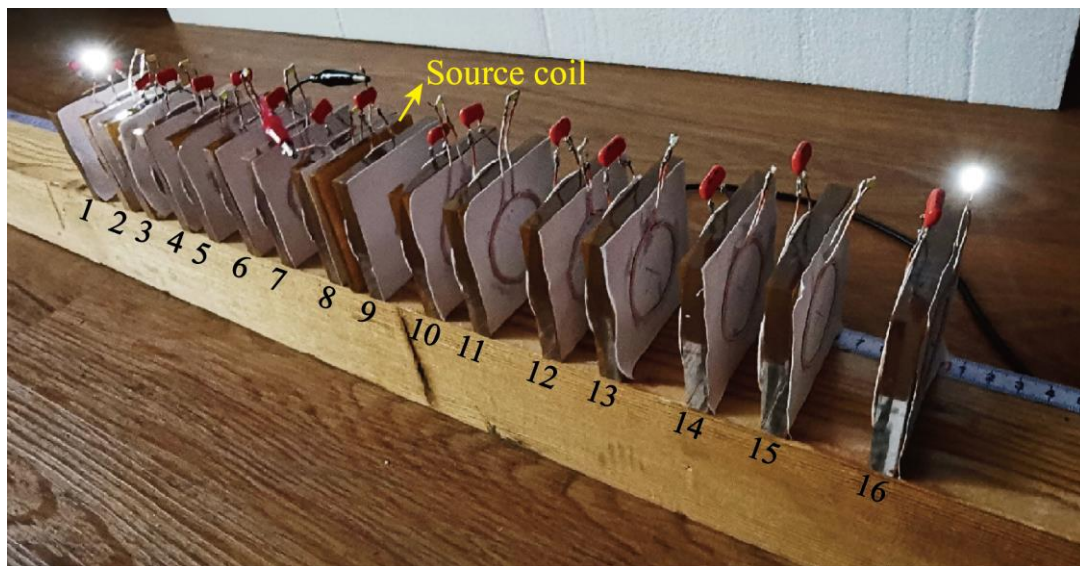


**FIG. 5. Experimental demonstration of the 1-w wireless power transfer for lighting two LED lamps.** The source non-resonant coil is placed on the center of the chain. To show the topological WPT intuitively, except for the two resonators near the source coil, all other resonators are added with LED lamps. At the working frequency  $f = 5.62$  MHz, the topological edge state can obviously light up the LED lamps on both sides of the chain, while the LEDs lamps loaded on other composite resonators remain dark.

## CONCLUSION

In summary, based on the topological dimer chain composed of ultra-subwavelength coil resonators, we experimentally verify that the edge state is not affected by the inner disorder perturbation, and can achieve high efficient long-range WPT. Our results have applied topological states to WPT system, which has many advantages over traditional WPT devices, such as efficient long-range transmission, distance independence, immunity to internal disturbances, etc. Moreover, this work provides a versatile platform with topological protection, which has the potential to explore more versatile WPT devices with more complex structures including the trimer and quasiperiodic chains.

## ACKNOWLEDGMENTS

This work was supported by the National Key R&D Program of China (Grant No. 2016YFA0301101), the National Natural Science Foundation of China (NSFC; Grant Nos. 11774261, 11474220, and 61621001), the Natural Science Foundation of Shanghai (Grant Nos. 17ZR1443800 and 18JC1410900), the China Postdoctoral Science Foundation (Grant Nos. 2019TQ0232 and 2019M661605), and the Shanghai Super Postdoctoral Incentive Program.

## References

1. L. Lu, J. D. Joannopoulos, and M. Soljačić, Topological photonics, *Nat. Photon.* 8, 821 (2014).
2. Y. Wu, C. Li, X. Y. Hu, Y. T. Ao, Y. F. Zhao and Q. H. Gong, Applications of topological photonics in integrated photonic devices, *Adv. Opt. Mater.* 5, 1700357 (2017).
3. T. Ozawa, H. M. Price, A. Amo, N. Goldman, M. Hafezi, L. Lu, M. C. Rechtsman, D. Schuster, J. Simon, O. Zilberberg, and I. Carusotto, Topological photonics, *Rev. Mod. Phys.* 91, 015006 (2019).

4. A. B. Khanikaev, S. H. Mousavi, W. K. Tse, M. Kargarian, A. H. MacDonald, and G. Shvets, Photonic topological insulators, *Nat. Mater.* 12, 233-239 (2013).
5. Z. W. Guo, H. T. Jiang, Y. Long, K. Yu, J. Ren, C. H. Xue, and H. Chen, Photonic spin Hall effect in waveguides composed of two types of single-negative metamaterials, *Sci. Rep.* 7, 7742 (2017).
6. H. Jia, R. Zhang, W. Gao, Q. Guo, B. Yang, J. Hu, Y. Bi, Y. Xiang, C. Liu, S. Zhang, Observation of chiral zero mode in inhomogeneous three dimensional Weyl metamaterials, *Science* 363, 148 (2019).
7. Y. H. Yang, Z. Gao, H. R. Xue, L. Zhang, M. J. He, Z. J. Yang, R. Singh, Y. D. Chong, B. L. Zhang and H. S. Chen, Realization of a three-dimensional photonic topological insulator, *Nature* 565, 622 (2019).
8. M. Hafezi, E. A. Demler, M. D. Lukin, and J. M. Taylor, Robust optical delay lines with topological protection, *Nat. Phys.* 7, 907-912 (2011).
9. G. Q. Liang and Y. D. Chong, Optical resonator analog of a two dimensional topological insulator, *Phys. Rev. Lett.* 110, 203904 (2013).
10. Y. Ao, X. Y. Hu, Y. L. You, C. C. Lu, Y. L. Fu, X. Y. Wang, and Q. H. Gong, Topological phase transition in the non-Hermitian coupled resonator array, *Phys. Rev. Lett.* 125, 013902 (2020).
11. Z. W. Guo, Y. Sun, H. T. Jiang, Y. Q. Ding, Y. H. Li, Y. W. Zhang, H. Chen, Experimental demonstration of an anomalous Floquet topological insulator based on negative-index media, *arXiv:2006.12252* (2020).
12. A. P. Slobozhanyuk, A. N. Poddubny, A. E. Miroshnichenko, P. A. Belov, and Y. S. Kivshar, Subwavelength topological edge states in optically resonant dielectric structures, *Phys. Rev. Lett.* 114, 123901 (2015).

13. A. P. Slobozhanyuk, A. N. Poddubny, I. S. Sinev, A. K. Samusev, Y. F. Yu, A. I. Kuznetsov, A. E. Miroshnichenko, and Y. S. Kivshar, Enhanced photonic spin Hall effect with subwavelength topological edge states, *Laser & Photonics Rev.* 10, 656 (2016).
14. S. Kruk, A. Slobozhanyuk, D. Denkova, A. Poddubny, I. Kravchenko, A. Miroshnichenko, D. Neshev, and Y. Kivshar, Edge states and topological phase transitions in chains of dielectric nanoparticles, *Small* 13, 1603190 (2017).
15. C. W. Peterson, W. A. Benalcazar, T. L. Hughes, and G. Bahl, A quantized microwave quadrupole insulator with topologically protected corner states, *Nature* 555, 346 (2018).
16. Y. Li, Y. Sun, W. W. Zhu, Z. W. Guo, J. Jiang, T. Kariyado, H. Chen, and X. Hu, Topological LC-circuits based on microstrips and observation of electromagnetic modes with orbital angular momentum, *Nat. Commun.* 9, 4598 (2018).
17. J. C. Bao, D. Y. Zou, W. X. Zhang, W. J. He, H. J. Sun, and X. D. Zhang, Topoelectrical circuit octupole insulator with topologically protected corner states, *Phys. Rev. B* 100, 201406(R) (2019).
18. M. Xiao, Z. Q. Zhang, and C. T. Chan, Surface impedance and bulk band geometric phases in one-dimensional systems, *Phys. Rev. X* 4, 021017 (2014).
19. H. Wu and X. Hu, Scheme for Achieving a Topological photonic crystal by using dielectric material, *Phys. Rev. Lett.* 114, 223901 (2015)
20. X. D. Chen, W. –M. Deng, F. L. Shi, F. L. Zhao, M. Chen, and J. W. Dong, Direct observation of corner states in second-order topological photonic crystal slabs, *Phys. Rev. Lett.* 122, 233902 (2019).
21. B. Y. Xie, G. X. Su, H. F. Wang, H. Su, X. P. Shen, P. Zhan, M. H. Lu, Z. L. Wang, and Y. F. Chen, Visualization of higher-order topological insulating phases in two-dimensional dielectric photonic

- crystals, *Phys. Rev. Lett.* 122, 233903 (2019).
22. Q. S. Huang, Z. W. Guo, J. T. Feng, C. Y. Yu, H. T. Jiang, Z. Zhang, Z. S. Wang, and H. Chen, Observation of a topological edge state in the X-ray band, *Laser & Photon. Rev.* 13, 1800339 (2019).
23. Q. Wang, H. Xue, B. L. Zhang, and Y. D. Chong, Observation of protected photonic edge states induced by real-space topological lattice defects, *Phys. Rev. Lett.* 124, 243602 (2020).
24. Z. Q. Yang, Z. K. Shao, H. Z. Chen, X. R. Mao, and R. M. Ma, Spin-momentum-locked edge mode for topological vortex lasing, *Phys. Rev. Lett.* 125, 013903 (2020).
25. D. Xiao, M. C. Chang, and Q. Niu, Berry phase effects on electronic properties, *Rev. Mod. Phys.* 82, 1959 (2010).
26. M. Z. Hasan and C. L. Kane, Topological insulators, *Rev. Mod. Phys.* 82, 3045 (2010).
27. X. L. Qi and S. C. Zhang, Topological insulators and superconductors, *Rev. Mod. Phys.* 83, 1057 (2011).
28. W. P. Su, J. R. Schrieffer, and A. J. Heeger, Solitons in polyacetylene, *Phys. Rev. Lett.* 42, 1698 (1979).
29. N. Malkova, I. Hromada, X. Wang, G. Bryant, and Z. Chen, Observation of optical Shockley-like surface states in photonic superlattices, *Opt. Lett.* 34, 1633 (2009).
30. J. Jiang, Z. W. Guo, Y. Q. Ding, Y. Sun, Y. H. Li, H. T. Jiang, and H. Chen, Experimental demonstration of the robust edge states in a split-ring-resonator chain, *Opt. Express* 26, 12891 (2018).
31. J. Jiang, J. Ren, Z. W. Guo, W. W. Zhu, Y. Long, H. T. Jiang, and H. Chen, Seeing topological winding number and band inversion in photonic dimer chain of split-ring resonators, *Phys. Rev. B*

- 101, 165427 (2020).
32. F. Zangeneh-Nejad and R. Fleury, Disorder-induced signal filtering with topological metamaterials, *Adv. Mat.* 2001034 (2020).
33. Y. Hadad, J. C. Soric, A. B. Khanikaev, and A. Alù, Self-induced topological protection in nonlinear circuit arrays, *Nat. Electron.* 1, 178 (2018).
34. D. Smirnova, D. Leykam, Y. D. Chong, and Y. Kivshar, Nonlinear topological photonics, *Appl. Phys. Rev.* 7,021306 (2020).
35. S. Xia, D. Jukić, N. Wang, D. Smirnova, L. Smirnov, L. Tang, D. Song, A. Szameit, D. Leykam, J. Xu, Z. Chen, and H. Buljan, Nontrivial coupling of light into a defect: the interplay of nonlinearity and topology, *arXiv: 2005.13848* (2020).
36. H. Zhao, P. Miao, M. H. Teimourpour, S. Malzard, R. El-Ganainy, H. Schomerus and L. Feng, Topological hybrid silicon microlasers, *Nat. Commun.* 9, 981 (2018).
37. M. Parto, S. Wittek, H. Hodaei, G. Harari, M. A. Bandres, J. Ren, M. C. Rechtsman, M. Segev, D. N. Christodoulides, and M. Khajavikhan, Edge-mode lasing in 1D topological active arrays, *Phys. Rev. Lett.* 120, 113901 (2018).
38. C. Poli, M. Bellec, U. Kuhl, F. Mortessagne, and H. Schomerus, Selective enhancement of topologically induced interface states in a dielectric resonator chain, *Nat. Commun.* 6, 6710 (2015).
39. S. Weimann, M. Kremer, Y. Plotnik, Y. Lumer, S. Nolte, K. G. Makris, M. Segev, M. C. Rechtsman, and A. Szameit, Topologically protected bound states in photonic parity-time-symmetric crystals, *Nat. Mater.* 16, 433 (2017).
40. B. K. Qi, L. X. Zhang, and Li Ge, Defect states emerging from a non-Hermitian flatband of photonic zero modes, *Phys. Rev. Lett.* 120, 093901 (2018).

41. S. Longhi, Topological phase transition in non-Hermitian quasicrystals, *Phys. Rev. Lett.* 122, 237601 (2019).
42. W. Song, W. Z. Sun, C. Chen, Q. H. Song, S. M. Xiao, S. N. Zhu, and T. Li, Breakup and recovery of topological zero modes in finite non-Hermitian optical lattices, *Phys. Rev. Lett.* 123, 165701 (2019).
43. Z. W. Guo, T. Z. Zhang, J. Song, H. T. Jiang, and H. Chen, Sensitivity of topological edge states in a non-Hermitian dimer chain, *arXiv: 2007.04409* (2020).
44. A. Kurs, A. Karalis, R. Moffatt, J. D. Joannopoulos, P. Fisher, and M. Soljačić, Wireless power transfer via strongly coupled magnetic resonances, *Science* 317, 83 (2007).
45. M. Song, P. Belov, and P. Kapitanova, Wireless power transfer inspired by the modern trends in electromagnetics, *Appl. Phys. Rev.* 4, 021102 (2017).
46. S. Kim, J. S. Ho, and A. S. Poon, Midfield Wireless Powering of subwavelength autonomous devices, *Phys. Rev. Lett.* 110, 203905 (2013).
47. A. P. Sample, D. A. Meyer, and J. R. Smith, Analysis, experimental results, and range adaptation of magnetically coupled resonators for wireless power transfer, *IEEE Trans. Ind. Electron.* 58, 544 (2011).
48. Y. Urzhumov and D. R. Smith, Metamaterial-enhanced coupling between magnetic dipoles for efficient wireless power transfer, *Phys. Rev. B* 83, 205114 (2011).
49. Q. Wu, Y. H. Li, N. Gao, F. Yang, Y. Q. Chen, K. Fang, Y. W. Zhang, and H. Chen, Wireless power transfer based on magnetic metamaterials consisting of assembled ultra-subwavelength meta-atoms, *Europhys. Lett.* 109, 68005 (2015).
50. M. Z. Song, K. Baryshnikova, A. Markvart, P. Belov, E. Nenasheva, C. Simovski, and P.

Kapitanova, Smart table based on a metasurface for wireless power transfer, *Phys. Rev. Appl.* 11, 054046 (2019).

51. Y. Q. Chen, Z. W. Guo, Y. Q. Wang, X. Chen, H. T. Jiang, and H. Chen, Experimental demonstration of the magnetic field concentration effect in circuit-based magnetic near-zero index media, *Opt. Express* 28, 17064 (2020).

52. B. L. Cannon, J. F. Hoburg, D. D. Stancil, and S. C. Goldstein, Magnetic resonant coupling As a potential means for wireless power transfer to multiple small receivers, *IEEE Trans. Power Electron.* 24, 1819 (2009).

53. A. P. Sample, D. A. Meyer, J. R. Smith, and Experimental Results Analysis, And range adaptation of magnetically coupled resonators for wireless power transfer, *IEEE Trans. Ind. Electron.* 58, 544 (2011).

54. B. N. Wang, K. H. Teo, T. Nishino, W. Yerazunis, J. Barnwell, and J. Y. Zhang, Experiments on wireless power transfer with metamaterials, *Appl. Phys. Lett.* 98, 254101 (2011).

55. K. JinWook, S. Hyeon-Chang, K. Kwan-Ho, and P. Young-Jin, Efficiency analysis of magnetic resonance wireless power transfer with intermediate resonant coil, *IEEE Antennas Wireless Propag. Lett.* 10, 389 (2011).

56. J. S. Hoa, A. J. Yeha, E. Neofytoub, S. Kima, Y. Tanabea, B. Patlollab, R. E. Beyguib, and A. S. Y. Poon, Wireless power transfer to deep-tissue microimplants, *Proc. Natl Acad. Sci. USA* 111, 7974 (2014).

57. H. Mei and P. P. Irazoqui, Miniaturizing wireless implants, *Nat. Biotechnol.* 32, 1008 (2014).

58. H. Li, J. Li, K. Wang, W. Chen, and X. Yang, A maximum efficiency point tracking control scheme for wireless power transfer systems using magnetic resonant coupling, *IEEE Trans. Power*

Electron. 30, 3998 (2015).

59. A. Krasnok, D. G. Baranov, A. Generalov, S. Li, and A. Alù, Coherently Enhanced Wireless Power Transfer, *Phys. Rev. Lett.* 120, 143901 (2018).

60. C. Saha, I. Anya, C. Alexandru, and R. Jinks, Wireless power transfer using relay resonators, *Appl. Phys. Lett.* 112, 263902 (2018).

61. C. Badowich and L. Markley, Idle power loss suppression in magnetic resonance coupling wireless power transfer, *IEEE Trans. Ind. Electron.* 65, 8605 (2018).

62. J. L. Zhou, B. Zhang, W. X. Xiao, D. Y. Qiu, and Y. F. Chen, Nonlinear parity-time-symmetric model for constant efficiency wireless power transfer: Application to a drone-in-flight wireless charging platform, *IEEE Trans. Ind. Electron.* 66, 4097 (2019).

63. M. Sakhdari, M. Hajizadegan, and P. Y. Chen, Robust extended-range wireless power transfer using a higher-order PT-symmetric platform, *Phys. Rev. Res.* 2, 013152 (2020).

64. S. Assawaworrarit, X. F. Yu, and S. H. Fan, Robust wireless power transfer using a nonlinear parity-time-symmetric circuit, *Nature* 546, 387 (2017).

65. G. Lerosey, Applied physics: Wireless power on the move, *Nature* 546, 354 (2017).

66. S. Assawaworrarit and S. H. Fan, Robust and efficient wireless power transfer using a switch-mode implementation of a nonlinear parity-time symmetric circuit, *Nat. Electron.* 3, 273 (2020).

67. Z. W. Guo, H. T. Jiang, Y. Sun, Y. H. Li, and H. Chen, Asymmetric topological edge states in a quasiperiodic Harper chain composed of split-ring resonators, *Opt. Lett.* 43, 5142 (2018).

68. X. L. Liu and G. S. Agarwal, The new phases due to symmetry protected piecewise berry phases; enhanced pumping and nonreciprocity in trimer lattices, *Sci. Rep.* 7, 45015 (2017).